SERI/TP-252-2976
UC Category: 62a
DE87001119

Analytical Model of an Irrigated Packed-Bed Direct-Contact Heat Exchanger at High Temperature

Mark S. Bohn

November 1986

Prepared for the Second ASME/JSME
Thermal Engineering Conference
Honolulu, Hawaii
22-27 March 1987

Prepared under Task No. 5122.210
FTP No. 5-651

Solar Energy Research Institute
A Division of Midwest Research Institute

1617 Cole Boulevard
Golden, Colorado 80401-3393

Prepared for the
U.S. Department of Energy
Contract No. DE-AC02-83CH10093

Printed in the United States of America
Available from:
National Technical Information Service
U.S. Department of Commerce
5285 Port Royal Road
Springfield, VA 22161

Price: Microfiche A01
Printed Copy A02

Codes are used for pricing all publications. The code is determined by the number of pages in the publication. Information pertaining to the pricing codes can be found in the current issue of the following publications, which are generally available in most libraries: *Energy Research Abstracts, (ERA); Government Reports Announcements* and Index (*GRA* and I); *Scientific and Technical Abstract Reports (STAR);* and publication, NTIS-PR-360 available from NTIS at the above address.

ABSTRACT

This paper presents an analytical model of direct-contact heat exchange (DCHX) in an irrigated packed bed at high temperatures. The specific application is heat exchange between molten salt and air where the molten salt is a sensible heat storage medium and high temperature air is required for an end process. The model defines several heat transfer mechanisms between the three components in the bed--the liquid, the gas, and the packing. It also includes the effect of conduction in the packing. Correlations found in the literature are used to calculate the associated heat transfer coefficients. The model is restricted to liquids that wet the packing material and to gas/liquid flow rates below the loading point. Three dimensionless equations describe the heat balance between the three bed components. The resulting dimensionless parameters reveal that for commercial DCHX systems, radiation heat transfer is unimportant relative to the convective heat transfer, which is consistent with previous experimental results for air/mercury and nitrogen/molten lead systems. The model also predicts volumetric heat transfer coefficients of about 10,000 W/m^{3}K, which is consistent with experimental work.

NOMENCLATURE

a	surface area per unit volume (m^{-1})
A_c	cross section area of empty column (m^2)
a_d	dry surface area per unit volume (m^{-1})
A_f	fin cross-sectional area (m^{-2})
C_1	constant in equation (2)
C_p	gas specific heat (J/kg K)
C_ℓ	liquid specific heat (J/kg K)
D	mass diffusivity (m^2/s)
d_p	characteristic packing dimension (m)
d_{pw}	packing diameter as defined by Whitaker (m)
dQ	local differential heat transfer in bed (W)
dV	incremental volume of bed (m^3)
f_d	fraction of dry surface area = $1 - a_w/a_p$
F	defined in equation (14)
Fr_ℓ	liquid film Froude number $a_p L^2/\rho_\ell{}^2 g$
$F_{\ell p}$	view factor, liquid to packing
G	gas loading = $\dot{m}_g/A_c$ (kg/m^2 s)
g	acceleration of gravity (m/s^2)
H_c	column height (m)
h	heat transfer coefficient (W/m^2 K)
h_p	height of the packing element (m)
h_r	radiation heat transfer coefficient (W/m^2 K)
h_w	heat transfer coefficient from Whitaker's correlation, equation (5) (W/m^2 K)
k_c	bed thermal conductivity (W/m K)
k_g	gas-side mass transfer coefficient (kg mol/h m^2 atm)
k_g	thermal conductivity of gas (W/m K)
k_ℓ	liquid-side mass transfer coefficient (m^3/s^3)
k_p	thermal conductivity of packing (W/m K)
k_{rb}	effective-bed thermal conductivity, equation (13) (W/m K)
$k_{r\ell}$	liquid-to-liquid radiation thermal conductivity (W/m K)
L	liquid loading = $\dot{m}_\ell/A_c$
L_f	fin length (m)
M	molecular weight (kg/kg mol)
	mass flow rate (kg/s)
m	defined in equation (7)
N_d	number of fins per unit volume (m^{-3})
N_R	number of packing elements per unit volume (m^{-3})
P	absolute pressure (atm)
P	fin perimeter (m)
Pr	Prandtl number
q_f	fin heat transfer (W)
R	gas constant (m^3 atm/K kg mol)
Re_ℓ	liquid film Reynolds number = $L/a_p\mu_\ell$
Re_g	gas Reynolds number = $6G/a_p\mu_g$
Re_{a_p}	Reynolds number as defined by Whitaker, equation (6)
Re_{ff}	falling-film Reynolds number, equation (9)
Sc	Schmidt number
T	temperature (K)

SERI

t_p	thickness of packing material (m)
Ua	volumetric heat transfer coefficient (W/m^3 deg C)
V_p	packing volume (m^3)
We_ℓ	liquid film Weber number = $L^2/\rho_\ell \sigma a_p$
x	axial distance (m)
$\bar{x}$	dimensionless axial distance

Greek

Γ	mass flow per unit width (kg/m s)
ε_ℓ	liquid emissivity
ε_p	packing emissivity
ε_v	packing void fraction
θ	dimensionless temperature
$\lambda_1, \lambda_2, \lambda_3, \ldots, \lambda_7$	dimensionless parameters
μ	viscosity (kg/ms)
ρ	density
σ	Stefan-Boltzman constant ($W/m^2\ K^4$)
σ	liquid surface tension (N/m)
σ_c	critical surface tension (N/m)

Subscripts

b	bed
e	effective or wet
ff	falling film
g	gas
i	inlet
ℓ	liquid
p	packing
r	radiative
ℓpr	liquid-to-packing, radiative
w	wetted

INTRODUCTION

Direct contact is an important mechanism for transferring mass between one fluid stream and another in industrial processes. Examples of such processes include gas-liquid contacting for absorption, humidification, and stripping. Direct contact may also be used to effect heat transfer between two fluid streams, if that contact does not cause undesired chemical reactions and if the streams can be separated afterwards. Direct-contact heat exchange (DCHX) is a potentially cost-effective method of transferring heat between such fluid streams primarily because it creates a very high surface area per unit volume. Additionally, intervening surfaces that exist for a conventional heat exchanger are not present. This increases the thermodynamic efficiency of the heat transfer process and further reduces the cost of the heat exchanger.

Because of the constraints on fluid stream compatibility, industry has exploited relatively few DCHX applications. One important exception is the heat transfer between molten salt and air in solar thermal central receiver applications. Here, the salt acts as a heat transfer fluid in the receiver and as a storage medium. The DCHX can provide high temperature air to an industrial process or to a turbine from the solar thermal energy stored in the salt. Conventional heat exchange uses a finned-tube heat exchanger. In a study of the comparative economics, Bohn (1) showed that the DCHX would be from 2 to 5 times more cost effective than a finned-tube exchanger, depending on the service temperature.

The particular DCHX configuration we are interested in is one in which counterflowing streams of a gas and a liquid enter a packed bed. As the liquid flows downward by gravity over the packing elements (rings, spheres, saddles, etc.), it is dispersed over the relatively large surface-area-per-unit volume of the packing element. Gas, flowing upward, contacts the liquid and the packing, and heat is transferred at the interface between the gas and liquid phases. In addition, radiation heat transfer may be important at high temperature.

This paper presents a model for predicting the performance of such a DCHX, in particular, at high temperature and with emphasis on the air and molten salt system. An accurate and reliable DCHX model would allow commercial units to be designed with confidence and also allow new units to be scaled from existing ones. Developing such a model would lead to a better understanding of the mechanisms of heat transfer and would allow us to differentiate between the important and unimportant mechanisms.

BACKGROUND

Few available models of direct-contact heat exchange involve all aspects of this problem, namely, simultaneous liquid and gas flow (irrigated bed), low-pressure-drop commercial packings, high-temperature operation, and molten-salt working fluids with properties that differ substantially from liquids typically used in irrigated packed-bed experiments.

Balakrishnan and Pei (2,3) developed a model of heat exchange between a gas and spherical particles in a packed bed. Dixon (4) modeled the thermal resistance of a packed bed with gas flow and used a simplified way to include radial terms. Huang (5) presented experimental data on direct-contact heat exchange between air and mineral spirits for Raschig rings, Intalox saddles, Pall rings, and HyPak rings. Standish (6) measured heat transfer between hot gases and mercury or cerrobend at low temperatures (up to 105 deg C) in an irrigated packed bed. Mackey and Warner (7) investigated a packed bed with counterflowing gas and liquid metals.

Although the work by Mackey and Warner is useful for liquid metal-gas systems, it is not sufficiently general to apply to other systems. For example, their direct mechanism, which was estimated from mass transfer data, is not applicable to molten salts because salt-vapor mass-transfer coefficients have not been measured (because of their exceedingly low vapor pressures and because their vapors are unimportant to industry). Moreover, Mackey and Warner's equations for heat transfer do not allow us to determine when radiation is important or why the different packing materials contributed differently to the direct and indirect mechanisms.

The model discussed here incorporates each heat-transfer mechanism individually rather than lumping them into an overall heat-transfer coefficient as done previously. Correlations available in the literature are used to calculate each heat transfer rate. Then, overall volumetric heat-transfer coefficients can be calculated. We have attempted to keep the model as general as possible. However, specific references to molten salt are required occasionally because of its unusual properties and our special interest in them. More details of the model development may be found in Bohn (8).

HEAT-TRANSFER MECHANISMS

The flow of liquid and gas in the packed bed was described qualitatively earlier, clearly indicating that modeling the heat-transfer process must involve several mechanisms. These mechanisms are (1) convection at the liquid-gas interface, (2) convection between the gas and the dry packing surface, (3) conduction in the packing element, (4) convection between the liquid and the packing surface on which the liquid is flowing, (5) radiation between portions of the dry packing, (6) conduction between packing elements, (7) radiation between portions of the liquid film, and (8) radiation from liquid to the packing.

Each heat-transfer mechanism needs to be expressed on a volumetric basis. That is, those mechanisms that occur at a surface will be expressed as a product of a surface heat-transfer coefficient and the surface area per unit volume over which the mechanism is active.

Convection at the Liquid-Air Interface

Mechanism 1 represents heat transfer at the interface between liquid and gas in the bed. Thus, we need to know the interfacial surface area as well as the film coefficients on the liquid and on the gas side of the interface. Onda et al. (9) developed a correlation that allows us to predict the fraction of packing area that will be wet by a liquid in a packed bed:

$$\frac{a_w}{a_p} = 1 - \exp\left[-1.45\ Re_\ell^{0.1}\ Fr_\ell^{-0.05}\ We_\ell^{0.2}\ \left(\frac{\sigma}{\sigma_c}\right)^{-0.75}\right] \tag{1}$$

for

$$\begin{aligned} 0.04 &< Re_\ell < 500 \\ 2.5\times10^{-9} &< Fr_\ell < 1.8\times10^{-2} \\ 1.2\times10^{-8} &< We_\ell < 0.27 \\ 0.3 &< \sigma/\sigma_c < 2.0 \ . \end{aligned}$$

For the flow rates of interest and properties of molten carbonate salts on oxidized metal, this correlation gave a 40%-60% range of wet surface area.

Because of a lack of heat-transfer data or correlations that could be applied directly to the salt and air interfacial convection problem, we will follow others (1,5,10) and apply the mass-transfer/heat-transfer analogy. We therefore require a mass transfer correlation to determine the heat transfer at the liquid-gas interface. One such correlation is that of Onda, Takeuchi, and Okumoto (11). The correlation equations for gas-side and liquid-side mass transfer coefficients are

$$k_g\left(\frac{RT}{a_p D_g}\right) = C_1\left(\frac{Re_g}{6}\right)^{0.7}\left(Sc_g\right)^{1/3}\left(a_p d_p\right)^{-2}$$

$$k_\ell\left(\frac{\rho_\ell}{g\mu_\ell}\right)^{1/3} = 0.0051\left(\frac{L}{a_w\mu_\ell}\right)^{2/3}\left(Sc_\ell\right)^{-1/2}\left(a_p d_p\right)^{0.4} \ . \tag{2}$$

The constant C_1 is equal to 2.0 for packing smaller than 15 mm, otherwise C_1 = 5.23.

To determine the gas-side heat-transfer coefficient, we have from the mass-transfer/heat-transfer analogy

$$\frac{h_g a}{C_p G} = \left(\frac{Sc_g}{Pr_g}\right)^{2/3}\left(\frac{k_g a_e P M_g}{G}\right) \ . \tag{3}$$

The power on the Schmidt number-Prandtl number ratio in equation (3) is 2/3, as recommended by Bravo and Fair (12). Applying equation (3) to the Onda correlation, we find for the dimensionless gas-side heat-transfer coefficient that

$$\frac{h_g a}{C_p G} = \frac{C_1}{Pr_g^{2/3}}\left(\frac{a_e a_p \mu_g}{G}\right)\left(\frac{Re_g}{6}\right)^{0.7}\left(a_p d_p\right)^{-2} \ . \tag{4}$$

In practice, the liquid-side film coefficient is about two orders of magnitude greater than the gas-side coefficient. Therefore, we will neglect the liquid-side resistance. For molten salt flow rates and properties of interest, equation (4) gives volumetric heat-transfer coefficients, $ha_{g\ell}$, in the range of 2000 to 5000 W/m^3 K.

Convection Between the Gas and the Dry Packing Surface

Mechanism 2 represents the transfer of heat from dry portions of the packing to or from the gas. It is important because the liquid rivulets flowing across the packing surface do not totally cover the packing surface area, yet can heat the dry areas by conduction. The gas flowing over the dry areas can then transfer heat from the dry surface. The conduction effect is treated in the next section.

Convective heat transfer from dry packed beds was studied extensively because of industrial interest in packed catalytic bed reactors, energy storage rock beds, and others. In these studies the main interest is the transfer of heat between the surface of the packing and the gas stream flowing over it. Whitaker (13) has compiled data from five sources and developed a correlation applicable to the present problem:

$$\frac{h_w d_{pw}}{k_g}\left(\frac{\varepsilon_v}{1-\varepsilon_v}\right) = Pr_g^{1/3}\left(0.5\ Re_{a_p}^{1/2} + 0.2\ Re_{a_p}^{2/3}\right) \tag{5}$$

for

$$10 < Re_{a_p} < 10000 \ .$$

The Reynolds number is defined as

$$Re_{a_p} = \frac{d_{pw} G}{\mu_g (1-\varepsilon_v)} \ . \tag{6}$$

The use of equation (5) for the problem of interest here neglects any effect on the heat-transfer caused by the interaction between the liquid film and the gas flowing over it.

For typical flow rates and property values, equation (5) gives local surface heat-transfer coefficients of about 70 W/m^2 K. If the packing were totally dry, this would be equivalent to a volumetric heat-transfer coefficient of 23,800 W/m^3 K for 5/8 in. Pall rings.

Conduction in the Packing Element

Several researchers (5,7,8) have recognized heat-transfer mechanism 3 as a possible reason why mass transfer correlations tend to underpredict heat-transfer data. This is because conduction through the packing allows the transfer of heat from wet areas to dry areas where the heat can be subsequently transferred to the gas stream. No comparable mechanism exists for mass transfer. To assess the magnitude of this effect and to determine if it can improve results calculated from mass transfer data, we developed a model based on conduction through and convection from a fin.

Consider Fig. 1, which depicts a packing element with liquid rivulets flowing down its surface. The flow of heat in the packing material and subsequent transfer to the surrounding gas flow is analogous to

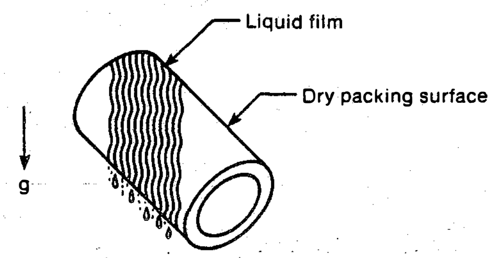

Fig. 1. Packing Element with Liquid Film

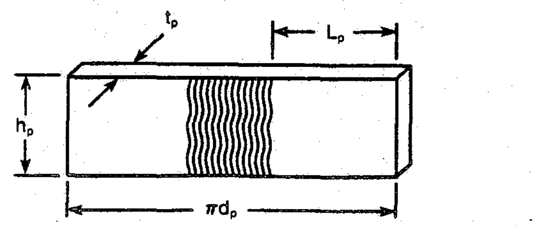

Fig. 2. Idealized Version of Packing Element with Liquid Film

the transfer of heat from a body with fins to a gas flow. Heat is transferred from the root of the fin by conduction and then by convection to the gas stream. Consider Fig. 2 as an idealization of Fig. 1.

An analysis of the fin effect is available in most heat-transfer textbooks, Kreith and Bohn (14) for example. Such an analysis gives the rate of heat transfer from each fin as

$$q_f = (hPk_pA_f)^{1/2}(T_p - T_g)\tanh(mL_f) ,$$

where

$$m = (hP/k_pA_f)^{1/2} .$$

To convert this expression to a volumetric basis, consider that the number of such fins per unit volume is

$$N_d = \frac{\text{dry surface area per unit volume}}{\text{dry surface area per fin}} = \frac{a_p - a_w}{L_fP}$$

Since $ha_{gp} = N_dq_f$, we have

$$ha_{gp} = (hPk_pA_f)^{1/2}\tanh(mL_f)\left(\frac{a_p - a_w}{L_fP}\right) \quad (7)$$

The heat-transfer coefficient in equation (7) is the one at the fin surface and therefore can be replaced by h_w from equation (5). The fin perimeter, P, heat flow cross-sectional area, A_f, and fin length, L_f, require careful definition in the case of the partially wet packing element for each type of packing. For Raschig rings we find

$$P = \frac{1}{2}[2(t_p + h_p)\ \pi d_p] \qquad A_f = \frac{1}{2}(h_pt_p + \pi d_pt_p) \quad (8)$$

$$L_f = \frac{f_d}{4}(\pi d_p + h_p) .$$

For typical flow rates and properties consistent with those used previously to give estimated heat-transfer coefficients, ha_{gp} will be 8900 W/m^3 K. This reduces the coefficient from 23,800 W/m^3 K for the completely dry packed bed is a result of a 50% reduction in dry surface area caused by rivulets and the 75% fin efficiency for these conditions.

Convection Between the Liquid Film and the Packing Surface

Mechanism 4 involves the transfer of heat from the liquid film to the surface of the packing. A great deal of work was done on falling film heat-transfer primarily because of the interest in condensers and falling film evaporators. We chose an analysis by Dukler (15) for falling film heat transfer that correlates heat transfer as a function of film Reynolds number:

$$Re_{ff} = \frac{4\Gamma}{\mu_\ell} , \quad (9)$$

where Γ is the mass flow of liquid divided by the wet perimeter. This can be estimated from

$$\Gamma \cong \frac{L}{\pi d_p^2 N_R(a_w/a_p)} , \quad (10)$$

yielding a Reynolds number of about 2.2 when L = 10 kg/m^2 s. For Reynolds numbers below about 1000, Dukler's analysis gives

$$h_{ff}\left(\frac{\mu_\ell^2}{\rho_\ell^2 g k_\ell^3}\right)^{1/3} = 0.36 . \quad (11)$$

On a volumetric basis, then, we have

$$ha_{\ell p} = h_{ff}a_w . \quad (12)$$

Radiation Between Portions of the Dry Packing and Conduction Between Packing Elements

These two mechanisms exist even when the bed has no liquid or gas flowing through it. Mechanism 5 is the transfer of heat by radiation from one dry area on a packing element to another at a different temperature. Mechanism 6 is the transfer of heat by conduction through the packing elements at the point of contact with other packing elements.

We chose the effective thermal conductivity method for modeling mechanisms 5 and 6. Schotte (16) presents a model for effective thermal conductivity of a dry packed bed:

$$k_{rb} = \frac{1 - \varepsilon_v}{\frac{1}{k_p} + \frac{1}{h_rd_p}} + \varepsilon_vh_rd_p + k_c , \quad (13)$$

where

$$h_r = 0.1952\varepsilon_p\frac{T_p^3}{10^6}\left(1 - \frac{a_w}{a_p}\right) .$$

The first term in equation (13) represents radiation to the packing in series with conduction through the packing, the second term represents radiation across void spaces between the packing elements, and the third term represents the conduction component [taken from Fig. 1 of Schotte (16)].

Radiation Between Portions of the Liquid Film

Portions of the liquid film see (have a nonzero view factor with) other parts of the liquid film and thus may transfer heat by radiation (mechanism 7). This may be calculated similarily to mechanism 5 without the conduction terms as derived by Schotte (16):

$$k_{r\ell} = 0.1952 d_p \varepsilon_\ell \frac{T_\ell^3}{10^6} \frac{a_w}{a_p} .$$

Radiation Between the Liquid and Dry Packing Surface

Finally, the liquid film and dry portions of the packing surface see one another and exchange heat by radiation (mechanism 8). Considering that the liquid film may only see other parts of the liquid film or dry packing surface areas and since the liquid film and the packing temperatures are close, the volumetric heat-transfer coefficient for radiation between the liquid film and the packing is

$$ha_{\ell pr} = \frac{4\sigma T_\ell{}^3}{F} , \tag{14}$$

where

$$F = \frac{1 - \varepsilon_\ell}{\varepsilon_\ell a_w} + \frac{1}{a_w F_{\ell p}} + \frac{1 - \varepsilon_p}{\varepsilon_p a_d} .$$

HEAT-TRANSFER EQUATIONS

We incorporate the heat-transfer mechanisms previously discussed into a one-dimensional model in the dimension parallel to the liquid and gas flow. We consider pure counterflowing gas and liquid, i.e., no backmixing, and consider that three "continuous" phases exist in the bed: gas, liquid, and the packing. Further, we will neglect radial heat losses out the column wall, assume that the inlet gas and liquid temperatures are known, and assume that the gas is transparent to radiation.

Consider Fig. 3 in which the packed bed is shown schematically. The bed was divided into elements of thickness, Δx, in the flow direction, x. At the top of the element, liquid enters at temperature $T_\ell(x + \Delta x)$, and gas exits at temperature $T_g(x + \Delta x)$. At the bottom of the element, liquid exits at temperature $T_\ell(x)$ and gas enters at temperature $T_g(x)$. In the bed element, Δx, the average temperature of the packing is $T_p(x)$.

An equation describing a heat balance on the liquid in the element Δx is derived based on heat transfer to the packing and the gas via the mechanisms discussed earlier. In differential form this becomes

$$LC_\ell \frac{dT_\ell}{dx} + k_{r\ell} \frac{d^2T_\ell}{dx^2} + (T_g - T_\ell)ha_{\ell g} + (T_p - T_\ell)ha_{\ell p} = 0 . \tag{15}$$

A similar equation expressing a heat balance on the gas in the element is

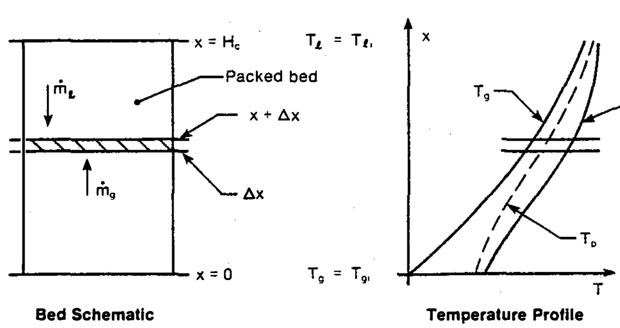

Fig. 3. Schematic of Bed for Development of Model

$$GC_{pg} \frac{dT_g}{dx} + (T_g - T_\ell)ha_{\ell g} + (T_g - T_p)ha_{gp} = 0 . \tag{16}$$

The equation expressing a heat balance on the packing is

$$k_{rb} \frac{d^2T_p}{dx^2} + (T_g - T_p)ha_{gp} + (T_\ell - T_p)ha_{\ell p} = 0 . \tag{17}$$

These equations can be made dimensionless with the following scaling:

$$\tilde{x} = x/H_c \qquad \theta_g = T_g/T_{\ell i}$$

$$\theta_\ell = T_\ell/T_{\ell i} \qquad \theta_p = T_p/T_{\ell i} .$$

The dimensionless form of the heat-transfer equations then become

$$\frac{d^2\theta_\ell}{d\tilde{x}^2} + \lambda_1 \frac{d\theta_\ell}{d\tilde{x}} + \lambda_2(\theta_g - \theta_\ell) + \lambda_3(\theta_p - \theta_\ell) = 0$$

$$\frac{d\theta_g}{d\tilde{x}} + \lambda_4(\theta_g - \theta_\ell) + \lambda_5(\theta_g - \theta_p) = 0 \tag{18}$$

$$\frac{d^2\theta_p}{d\tilde{x}^2} + \lambda_6(\theta_g - \theta_p) + \lambda_7(\theta_\ell - \theta_p) = 0$$

All the heat-transfer coefficients, dimensions, flow rates, and property values were incorporated into seven dimensionless groups, which are

$$\lambda_1 = \frac{LC_\ell H_c}{k_{r\ell}} = \frac{\text{enthalpy via liquid mass flux}}{\text{enthalpy via radiation}}$$

$$\lambda_2 = \frac{ha_{\ell g} H_c{}^2}{k_{r\ell}} = \frac{\text{gas-liquid convection}}{\text{liquid-liquid radiation}}$$

$$\lambda_3 = \frac{ha_{\ell p} H_c{}^2}{k_{r\ell}} = \frac{\text{liquid-packing convection/radiation}}{\text{liquid-liquid radiation}}$$

$$\lambda_4 = \frac{ha_{g\ell} H_c}{GC_p} = \frac{\text{gas-liquid convection}}{\text{enthalpy via gas mass flux}}$$

$$\lambda_5 = \frac{ha_{gp} H_c}{GC_p} = \frac{\text{gas-packing convection}}{\text{enthalpy via gas mass flux}}$$

$$\lambda_6 = \frac{ha_{gp} H_c{}^2}{k_{rb}} = \frac{\text{gas-packing convection}}{\text{packing radiation}}$$

$$\lambda_7 = \frac{ha_{\ell p} H_c{}^2}{k_{rb}} = \frac{\text{liquid-packing radiation and convection}}{\text{packing radiation}} .$$

We determined the magnitude of the seven dimensionless groups by using the previously discussed correlations for $k_{r\ell}$, $ha_{\ell g}$, etc., for three cases: conditions typical of an experimental-size DCHX with air/molten carbonate salt at 500 deg C, conditions typical of a commercial-size DCHX with air/molten carbonate salt at 900 deg C, and conditions typical of an advanced commercial-size DCHX operating at 1100 deg C. For all three cases we find that all λ are >>1 with the exception of λ_4 and λ_5, which are O(1). This means that the heat transfer by radiation, even at very high temperatures with commercial-size packing, is negligible relative to the convective terms. Therefore, we drop the radiative terms in equation (18). In addition, the equation expressing the heat balance in the packing may be algebraically eliminated. This yields

$$\lambda_1\theta_\ell' + \lambda_2(\theta_g - \theta_\ell) + \lambda_3\left(\frac{\lambda_6}{\lambda_7 + \lambda_6}\right)(\theta_g - \theta_\ell) = 0$$

$$\theta_g' + \lambda_4(\theta_g - \theta_\ell) + \lambda_5\left(\frac{\lambda_7}{\lambda_7 + \lambda_6}\right)(\theta_g - \theta_\ell) = 0 \ , \qquad (19)$$

where

$$\theta' \equiv \frac{d\theta}{d\tilde{x}}$$

with the boundary conditions

$$\theta_g(0) = \theta_{gi} \quad \text{and} \quad \theta_\ell(1) = 1 \ .$$

We found that if we used the property values calculated at the mean temperature for each stream, the solution was very close to the variable property calculation. Therefore, we assume that the properties are constant.

Without the radiation terms and assuming constant properties, equation (19) simply describes heat transfer in a counterflow heat exchanger. It is a straightforward procedure to solve the equations if needed. However, the volumetric heat-transfer coefficient can be extracted from the differential equations with

$$Ua = \frac{dQ}{dV}\frac{1}{T_\ell - T_g} = T_{\ell i}\,\frac{LA_cC_\ell}{H_c}\,\frac{d\theta_\ell}{d\tilde{x}} \ .$$

Equation (19) may by manipulated to give an expression for $d\theta_\ell/d\tilde{x}$ resulting in

$$Ua = ha_{g\ell} + \frac{ha_{gp}ha_{\ell p}}{ha_{gp} + ha_{\ell p}} \ . \qquad (20)$$

Equation (20) simply states that the overall heat-transfer coefficient is composed of the liquid-gas thermal resistance in parallel with the series combination of the liquid-packing resistance and the gas-packing resistance.

To meet the requirement that the average of the inlet and outlet temperatures for each fluid stream be used to calculate the fluid properties, we used an iterative solution. Results can be given as Ua as a function of G, L, $T_{\ell i}$, and fluid and packing properties.

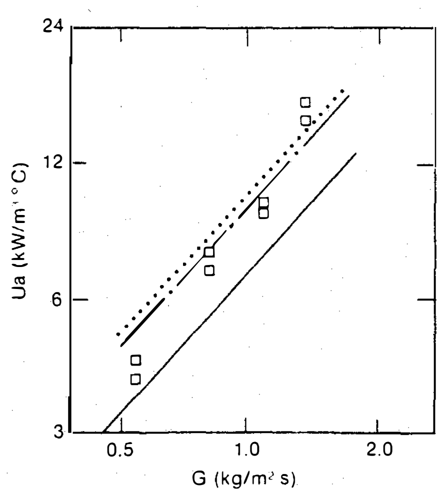

Fig. 4. Comparison of Present Model with Results of Huang, L = 2.71 kg/m²s □ Huang data, ——— Huang Model for $ha_{\ell g}$, — · — Present Model for $ha_{\ell g}$, ... Present Model for Ua, 1-1/2-in. Ceramic Raschig Rings

RESULTS

A comparison of the results of the present model with that of Huang (5) along with the data of Huang is shown in Figs. 4-7. In Figs. 4-6, the volumetric heat-transfer coefficient, Ua, is plotted against G with L held constant. In all these plots, we see that the results for $ha_{\ell g}$ (the convective heat-transfer at the liquid-gas interface that is to be compared with Huang's model) consistently agree better with Huang's data than Huang's model, even though the derivation for both models is based on the mass transfer analogy. We attribute the difference to our usage of a 2/3 power on the Schmidt-Prandtl number ratio in the mass-transfer/heat-transfer analogy and Huang's usage of a 1/2 power. Note, however, that neither model exhibits the same slope as the data; this suggests a more fundamental problem with using mass transfer data to predict heat transfer for packed beds.

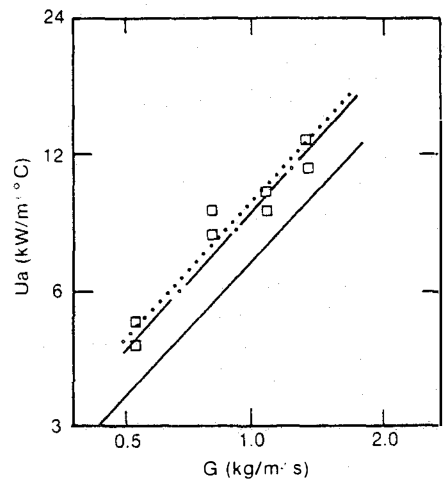

Fig. 5. Comparison of Present Model with Results of Huang, L = 2.71 kg/m²s □ Huang data, ——— Huang Model for $ha_{\ell g}$, — · — Present Model for $ha_{\ell g}$, ... Present Model for Ua, 1-1/2-in. Steel Pall Rings

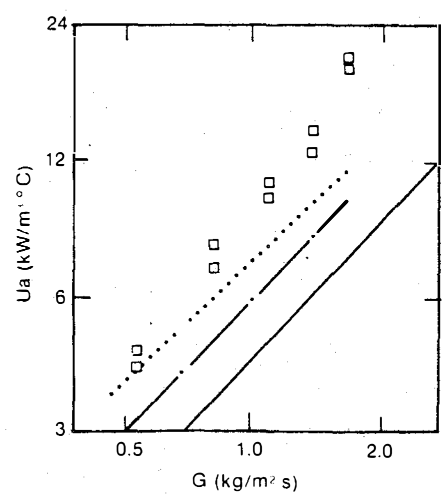

Fig. 6. Comparison of Present Model with Results of Huang, L = 2.71 kg/m²s □ Huang data, ——— Huang Model for $ha_{\ell g}$, — · — Present Model for $ha_{\ell g}$, ... Present Model for Ua, 1-1/2-in. Ceramic Intalox Saddles

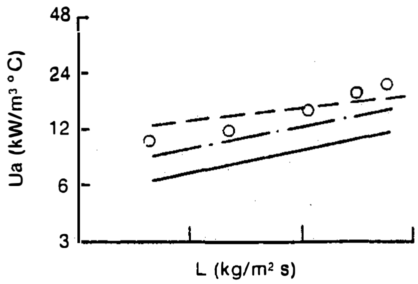

Fig. 7. Comparison of Present Model with Results of Huang, L = 2.71 kg/m^{2}s □ Huang data, ——— Huang Model for $ha_{\ell g}$, — · — Present Model for $ha_{\ell g}$, - - - Present Model for Ua.

For all three types and two sizes of packing [ceramic Raschig rings, carbon-steel Pall rings, and ceramic Intalox saddles, 1-in. (not shown here) and 1.5-in. sizes], the correction for conduction (see curve labeled Ua) in the packing further improves agreement between the present model for $H_{\ell g}$ and Huang's data. This correction is fairly small because the wet areas are a large fraction of the total packing area. Wet areas ranged from 80% to 90% of the packing area. Since the conduction correction is applied only over the dry area, the increase in heat-transfer area is small, e.g., 10% to 20% of the packing area. The correction for the Intalox saddles is the largest because the saddles exhibited the smallest wet area (80%-82%). The correction for the Pall rings is the smallest because the rings exhibited the largest wet area (86%-90%).

A comparison of the data and models at fixed G and variable L is shown in Fig. 7. Similar conclusions can be drawn here; e.g., the models do not predict the same sensitivity to L as do the data, general agreement is fairly good, and the present model with the conduction correction is an improvement over the original model by Huang (5).

Comparing the model results with Mackey's and Warner's (7) experimental results is a relatively severe test because their use of mercury prevented wetting of the packing altogether. Since our main interest is in applications where the packing is well wet, comparison of the model results with nonwetting data is mostly of academic interest. A problem with the comparison of interest here is determining the critical surface tension, σ_c. For the mercury system, which is nonwetting, we have $\sigma_c < \sigma$, but very little additional information is available. Thus, we were forced to use σ_c as a parameter for the comparison. The upper limit to σ_c is $\sigma = 0.48$ for mercury. For the range of σ_c from 0.1 to 0.4 N/m, we were not able to get reasonable agreement with Mackey's and Warner's data. Therefore, we conclude that since Onda's wetting correlation, equation (1), was not tested for very high surface tension liquids, its applicability and the applicability of the present model is limited to lower surface tension liquids, specifically those that wet the packing surface.

Another important conclusion from Mackey's and Warner's data is that the effect of radiation is negligible. Mackey and Warner compared results from the room temperature air/mercury system with results from their lead/nitrogen system at 450 deg C and found that Ua varied by less than 5% for this large temperature change. Thus, consistant with the analysis presented here, radiation heat transfer does not play an important role in an irrigated packed-bed DCHX.

Finally, we wish to report on preliminary measurements of Ua in an air-molten salt system at 550 deg C performed as a part of the work presented in this paper. A more detailed discussion of these experimental results will be presented in the near future.

Measurements were made in a 0.152-m inside diameter packed column with a 0.61-m bed height. The packing was oxidized 5/8-in. stainless steel Pall rings, and the salt was the eutectic of lithium-sodium-potassium carbonate (43.5%, 31.5%, 25.0%, molar, respectively), which melts at 397 deg C. Preheated air at 450 deg C was supplied by an electric air heater at the base of the column. A three-hole cannister liquid distributor fed from a single salt inlet pipe distributed the salt.

Figure 8 presents the results for experimental points at a fixed liquid rate and three air rates. Comparison with the model shows very good agreement for two of the points and reasonably good agreement with one point. The range of air flow tested here covers a large fraction of the actual column working range. In terms of liquid flow we need to test a range, especially lower liquid flows, although based on our previous work and results of others, L has a fairly weak effect on Ua. We also intend to test a range of temperatures to confirm a lack of effect of radiation heat transfer. Nevertheless, this preliminary set of data seems to confirm that the model can predict heat transfer in an irrigated packed-column DCHX with reasonable accuracy. Also note that the measured and predicted volumetric heat-transfer coefficients are about 3 to 4 times larger than we measured previously (1). Since our previous work concluded that DCHX was a very cost-effective technology for heating gases with liquids, results presented herein reinforce this conclusion and, in fact, show that DCHX is even more cost effective than previously thought.

CONCLUSIONS

We have presented a model of direct-contact heat exchange in an irrigated, packed bed operating at high temperatures. All modes of heat exchange were accounted for in the model, and each was modeled with correlations available in the literature. Most of these correlations were thoroughly tested and are based on a wide range of packing sizes, so we expect the model to be applicable to commercial-size heat exchangers. A dimensionless analysis reveals that for

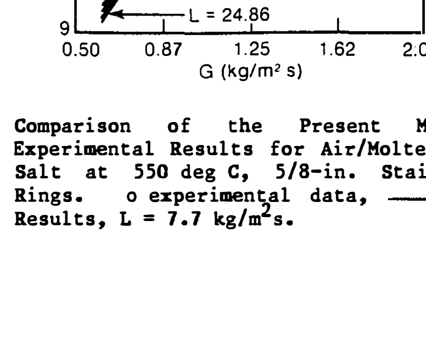

Fig. 8. Comparison of the Present Model with Experimental Results for Air/Molten Carbonate Salt at 550 deg C, 5/8-in. Stainless Pall Rings. o experimental data, ——— Model Results, L = 7.7 kg/m^{2}s.

SERI

such systems operating even at the highest temperatures, radiation heat transfer is not important compared with the convective heat transfer. The model also includes explicitly the packing conduction effect recognized by several researchers but was not previously modeled.

The unimportance of radiation heat transfer is confirmed by the data available in the literature. Comparison of the model with literature data also indicates that the model predicts more accurately the experimental data than do other models, and the correction for packing conduction further improves the comparison with the data. Usage of the model is not recommended for liquids that do not wet the packing. None of the mass-transfer-analogy-based models predict the sensitivity of Ua to L or G with great precision. This suggests a fundamental problem with using the analogy even though results of sufficient accuracy for engineering purposes are possible. Finally, comparison with experimental data for air and molten salt data at high temperatures indicates good agreement with the model for the restricted range of liquid flow rates tested.

REFERENCES

1. Bohn, M., "Air/Molten Salt Direct Contact Heat-Transfer," Journal of Solar Energy Engineering, Vol. 197, 1985, pp. 208-214.

2. Balakrishnan, A. R., and Pei, D. C. T., "Heat Transfer in Gas-Solid Packed Bed Systems. 2. The Conduction Mode," Ind. Eng. Chem. Process Des. Dev., Vol. 18, No. 1, 1979, pp. 40-46.

3. Balakrishnan, A. R., and Pei, D. C. T., "Heat Transfer in Gas-Solid Packed Bed Systems. 3. Overall Heat Transfer Rates in Adiabatic Beds," Ind. Eng. Chem. Process Des. Dev., Vol. 18, No. 1, 1979, pp. 47-50.

4. Dixon, A. G., "Thermal Resistance Models of Packed-Bed Effective Heat Transfer Parameters," AIChE Journal, Vol. 31, No. 5, 1985, pp. 826-834.

5. Huang, C., "Heat Transfer by Direct Gas-Liquid Contacting," M.S. Thesis, University of Texas at Austin, 1982.

6. Standish, N., "Heat Transfer in Liquid Metal Irrigated Packed Beds Countercurrent to Gases," Transactions of the Metallurgical Society of AIME, Vol. 242, 1968, pp. 1733-1740.

7. Mackey, P. J., and Warner, N. A., "Heat Transfer Between Dispersed Liquid Metals and Gases in Packed Beds," Metallurgical Transactions, Vol. 3, 1972, pp. 1807-1816.

8. Bohn, M., Modeling High-Temperature Direct-Contact Heat Exchange, SERI/TR-252-3056, Mar. 1987, Solar Energy Research Institute, Golden, Colo.

9. Onda, K., Takeuchi, H., and Koyama, Y., "Effect of Packing Materials on the Wetted Surface Area," Kagaku Kogaku, Vol. 31, No. 2, 1967, pp. 126-134.

10. Fair, J. R., "Designing Direct Contact Coolers/Condensors," Chemical Engineering, June 1972, pp. 91-100.

11. Onda, K., Takeuchi, H., and Okumoto, Y., "Mass Transfer Coefficients Between Gas and Liquid Phases in Packed Columns," J. Chemical Engineering of Japan, Vol. 1, 1968, pp. 56-62.

12. Bravo, J. L., and Fair, J. R., "Generalized Correlations for Mass Transfer in Packed Distillation Columns," Ind. Eng. Chem. Process Des. Dev., Vol. 21, 1982, pp. 162-170.

13. Whitaker, S. "Forced Convection Heat Transfer Correlations for Flow in Pipes, Past Flat Plates, Single Cylinders, Single Spheres, and for Flow in Packed Beds and Tube Bundles," AIChE Journal, Vol. 18, No. 2, 1972, pp. 361-371.

14. Kreith, F., and Bohn, M. S., Principles of Heat Transfer, 4th Ed., Harper and Row, New York, 1986.

15. Dukler, A. E., "Fluid Mechanics and Heat Transfer in Vertical Falling-Film Systems," Chem. Eng. Prog. Symp. Series, Vol. 56, No. 30, 1960, pp. 1-10.

16. Schotte, W. "Thermal Conductivity of Packed Beds," AIChE Journal, Vol. 6, No. 1, 1960, pp. 63-67.